Controlled Integration of Polymers into Viral Capsids

Marta Comellas-Aragonès, Andrés de la Escosura, A. (Ton) J. Dirks, Anne van der Ham, Anna Fusté-Cuñé, Jeroen J. L. M. Cornelissen,*,† and Roeland J. M. Nolte

Institute for Molecules and Materials, Radboud University Nijmegen, Heyendaalseweg 135, 6525 AJ, Nijmegen, The Netherlands

Received July 14, 2009; Revised Manuscript Received October 1, 2009

In this paper, we describe the controlled incorporation of two synthetic polymers with different structures in the cowpea chlorotic mottle virus (CCMV) capsid. Poly(ethylene glycol) (PEG) chains have been attached to the amine groups of lysine residues on the outer surface of the viral capsid. The functionalization of CCMV with PEG chains provoked a slow but irreversible dissociation of the virus into PEG-coat protein (CP) subunits, likely due to steric interference between the protein−protein subunits as a result of the presence of the PEG chains. This thermodynamic instability, however, can be overcome if a second polymer, such as polystyrene sulfonate (PSS), is present within the capsid. After complete disassembly of the PEG-CCMV conjugates and removal of the viral RNA, incubation of the PEG-functionalized coat proteins with PSS resulted in the formation of much more robust PSS-CCMV-PEG capsids with a diameter of 18 nm ($T = 1$ capsids). These are the first virus-like particles bearing synthetic organic polymers both inside and outside the viral capsid, opening a new route to the synthesis of biohybrid nanostructured materials based on viruses.

Introduction

Based on their reciprocal relationship, biology and chemistry are converging more and more into a new discipline called chemical biology. This discipline aims to understand biological issues at the chemical level, for instance, by the probing of biomolecules with synthetic compounds that interact with them. An opposite trend is also receiving much attention, namely, the use of well-defined biological structures and pathways that are used as a source of inspiration for the development of new materials and chemical processes, which have led to important advances in the fields of materials science and biotechnology.[1,2] Viruses are biological entities that, for the same reason that they exist, between nonliving and living matter, occupy a special position at the interface of chemistry and biology.[3] Although they are structurally complex, viruses do not have a metabolism of their own and their chemical machinery is relatively simple to manipulate. The size and shape of viruses, as well as the number and location of the functional groups on their inner and outer surfaces, are precisely defined. A new emerging field uses viruses as platforms for the controlled positioning of chemical species with different functions at the nanoscopic level.[4,5]

The outer decoration of both icosahedral and rod-like viruses using both genetic and chemical manipulation, has been extensively explored in the last years. A number of moieties including metal nanoparticles, fluorescent dyes, biotin, histidine tags, carbohydrates, DNA, peptides, proteins, conducting compounds, and luminiscent quantum dots have been incorporated onto a variety of viruses.[4−8] On the other hand, the hollow cavities of icosahedral viral capsids and other protein cages have been used as nanocontainers. Inorganic nanoparticles, for instance, can be easily synthesized by nucleating mineralization reactions inside nucleic acid-free viral capsids of different sizes.[9,10] The catalysis of organic reactions within these nanocontainers is also possible using previously encapsulated metal clusters,[11−14] palladium complexes,[15] and enzymes.[16]

In the same way as for natural polymers, that is, peptides and proteins,[17,18] the covalent attachment of synthetic organic polymers to the exterior surface of viruses is an interesting approach to broaden their applications in biomedicine and nanotechnology.[19] This strategy might improve the thermal stability of the viral cages. Synthetic polymers may also impart solubility in organic solvents and new self-assembling properties to the virus particles. Up until now, only three examples of the functionalization of viral capsids with synthetic polymers are known in the literature. The outer surfaces of the tobacco mosaic virus (TMV),[20] the cowpea mosaic virus (CPMV),[21−23] and the bacteriophage MS2[24] have been modified with poly(ethylene glycol) (PEG), and the resulting conjugates were found to display new solubility properties and altered immunogenicity, consistent with the known chemical and biological properties of PEG.[25,26]

The encapsulation of synthetic polymers inside viral capsids allows the formation of so-called virus-like particles (VLPs), which have the potential to be used as new building blocks for the preparation of nanostructured materials.[27] The large size of a macromolecule, however, requires that the virus particle displays the ability to reversibly disassemble/assemble to allow the polymer molecule to be encapsulated. One of the most widely studied viruses of this category is the cowpea chlorotic mottle virus (CCMV).[28] The icosahedral capsid of CCMV has an outer diameter of 28 nm and a well-defined inner cavity with a diameter of 18 nm. It is formed from 90 homodimers of 20 kDa coat protein (CP) subunits arranged with $T = 3$ Caspar-Klug symmetry around a central RNA strand. The CP consists of 189 amino acids with nine basic residues at the N-terminal RNA binding domain. An interesting property of the CCMV is its reversible disassembly/assembly behavior depending on the pH and ionic strength.[29] By varying these conditions, CCMV virions can be disassembled in vitro into protein dimers and, after removal of the RNA, reassembled again forming empty capsids. This pH-dependent behavior has been used to encap-

* To whom correspondence should be addressed. E-mail: j.j.l.m.cornelissen@tnw.utwente.nl.

† Present address: Laboratory for Biomolecular Nanotechnology, MESA+ Institute, University of Twente, Enschede, The Netherlands.

10.1021/bm9007953 CCC: $40.75
Published on Web 10/19/2009

Scheme 1. Schematic Pathway Towards PSS-CCMV-PEG Virus-like Particles

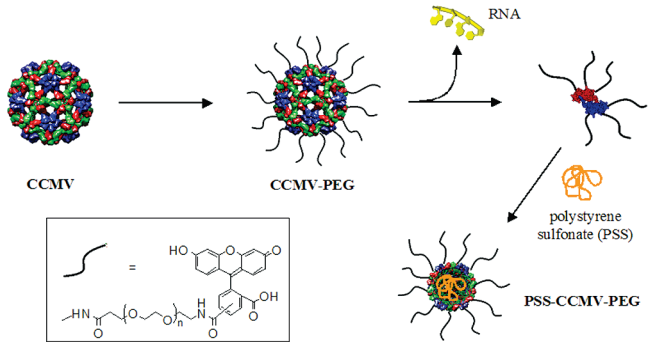

sulate a number of species such as proteins,[16] inorganic nanoparticles,[30,31] and polymers.[32,33]

Despite the fact that the CCMV capsid was assembled in vitro for the first time more than 40 years ago,[34] the mechanistic understanding of its assembly is still not completely clear, especially regarding the occurrence of polymorphism when the viral proteins are assembled in the presence of different types of cargoes. The CCMV coat protein can form, depending on the conditions, a variety of structures including tubes and icosahedral capsids with Caspar-Klug triangulation numbers of $T = 1$, 3, 4, and 7.[35,36] Inclusion of negatively charged polymers strongly influences the CP self-assembly process, giving rise to the formation of VLPs with only one of the above-mentioned symmetries. Polystyrene sulfonate (PSS), for example, is able to produce $T = 1$ particles at neutral pH[32] and particles with a $T = 2$ or 3 geometry at pH 5,[33] whereas tubular structures are obtained when double-stranded DNA is used as the polymeric cargo.[37] The covalent modification of CCMV protein subunits on the outer surface of viral capsids is also expected to alter their stability and assembly properties in a similar way as has been seen for other types of viruses.[38] This may be particularly relevant when organic polymers are used as decoration motifs, considering their own characteristic phase behavior. Understanding the interplay between the different effects that the incorporation of organic polymers, either inside the viral capsids or covalently attached to the outer surface, can provoke on the stability and assembly of such VLPs, appears to be a crucial factor in the design and preparation of virus-polymer hybrid materials.

As part of our efforts to develop methodologies that enable the precise positioning of different synthetic polymers in viral architectures, we describe here the controlled integration of PEG to the outer surface of the CCMV capsid and PSS into the inner cavity of the virus. Our strategy relies on the combined use of the assembly/disassembly properties of the viral protein and the successive incorporation of both polymers (Scheme 1). First, the native CCMV is modified by the covalent binding of PEG chains to the surface. At this stage the interfering functionalization of internal lysine and arginine residues is very unlikely because they strongly interact with the viral nucleic acid that is still present inside the capsids. After complete dissociation of the modified virus into protein subunits and precipitation of RNA, the addition of PSS resulted in the formation of VLPs. PSS does not only play the role of a guest during the encapsulation process but also acts as a template for the assembly. The electrostatic interactions between PSS and the positive N-terminus of the CPs are assumed to be the driving force to overcome the lower tendency of PEG-functionalized protein subunits to associate with each other at higher pH.

Experimental Section

Coupling of α-NHS Ester *ω*-Fluorescein Functionalized PEG-3000 (1; see Schemes 2 and S1) to CCMV. A CCMV solution (8.48 mg mL^{-1}, 2.5 mL) in sodium acetate buffer (0.05 M, 1.0 M NaCl, pH 5.0) was dialyzed against phosphate buffer (0.1 M, 0.001 M EDTA, pH 7.5) over a period of 9 h (with buffer changes every 3 h, $T = 4$ °C) using a 12−14 kDa MWCO dialysis membrane. Samples **A**−**D** with different CP/PEG (**1**) ratios (1:50 (**A**), 1:25 (**B**), 1:10 (**C**), and 1:1 (**D**)) were prepared by the addition of variable aliquots of a stock solution of compound **1** (0.081 M) in the same phosphate buffer to the CCMV solution (500 μL, 1.61 × 10^{-4} mmol; Table S1). Additional phosphate buffer was added, when necessary, to provide final volumes of 600 μL for all samples. A control sample was prepared in the same way as for sample **A** but using compound **2** (see Scheme S1) instead of **1**.

Samples **A**−**D** were incubated on a roller mixer for 2 h at room temperature and subsequently overnight at 4 °C. They were protected from light at all times. The excess of fluorescein-functionalized PEG was removed by size exclusion chromatography (SEC, Sephadex G-100) with the same phosphate buffer as eluent. The PEG-functionalized virus (orange in color) eluted before the excess of PEG (**1**; bright yellow). All fractions were analyzed by FPLC, SDS-PAGE, TEM, and UV/vis spectroscopy.

Isolation of the PEG-Functionalized CCMV Coat Protein (Removal of the Viral RNA). A purified PEG-functionalized CCMV solution (ca. 5 mg mL^{-1}, 1 mL; sample **C**) was extensively dialyzed overnight against Tris-HCl buffer (0.02 M, 1 M NaCl, 0.001 M DTT, pH 7.5) using a 6−8 kDa MWCO dialysis membrane. The solution was ultracentrifuged at 45000 rpm for 16 h at 4 °C. The top three-quarters of the supernatant was removed with a micropipet and analyzed by FPLC, SDS-PAGE, and UV/vis spectroscopy (see the Supporting Information, Figure S7). The nonfunctionalized coat protein obtained from CCMV, as described in the literature,[16,39,40] was used as a control.

Assembly of PSS-CCMV-PEG Virus-like Particles. Two different solutions of CP (600 μL, 0.82 mg mL^{-1}) and PEG-CP (300 μL, 1.20 mg mL^{-1}, isolated from sample **C**), both in the same Tris-HCl buffer (0.02 M, 1.0 M NaCl, 0.001 M DTT, pH 7.5), were dialyzed separately against phosphate buffer (0.1 M, 0.3 M NaCl, 0.001 M EDTA, pH 7.5). PSS ($M_n = 70000$, 17 mg, 2.42 × 10^{-4} mmol) was dissolved into the same phosphate buffer (170 μL) and diluted 50 times to obtain a PSS stock solution (2.86 × 10^{-5} M).

The assembly mixtures, containing different relative amounts of CP and PEG-CP (samples **E** (0% PEG-CP), **F** (25% PEG-CP), **G** (50% PEG-CP), **H** (75% PEG-CP), and **I** (100% PEG-CP)), were prepared by adding volumes of the stock solutions of both components, according to Table S2, to the PSS stock solution (20 μL, 1.94 × 10^{-4} mmol repeating units). A CP/PSS repeating unit ratio of approximately 1:40 was used in all cases. The samples were protected from light and incubated on a roller mixer for 30 min at room temperature, followed by storage at 4 °C. The characterization of samples **E**−**I** was performed by FPLC and agarose gel electrophoresis, and the purified FPLC fractions were further analyzed by fluorescence spectroscopy, TEM, SDS-PAGE, and agarose gel electrophoresis.

Results and Discussion

Formation of PEG-Functionalized CCMV. According to crystallographic data for the CCMV structure, there are, per subunit, four lysine groups accessible on the exterior surface, from which only three seem to be available for functionalization (Figure S1).[41,42] This abundance of reactive amine groups on the virus surface allows for facile and high yielding modification using *N*-hydroxysuccinimide (NHS) esters. Hence, the current study began with the synthesis of α-NHS ester *ω*-fluorescein functionalized PEG with $M_n = 3000$ Da (compound **1** in Scheme 2; Scheme S1). Labeling with a fluorescein moiety was used as a means to advance the characterization of the CCMV-PEG

Scheme 2. Functionalization of CCMV Surface-Exposed Amine Groups with α-NHS Ester ω-Fluorescein Functionalized PEG (**1**)

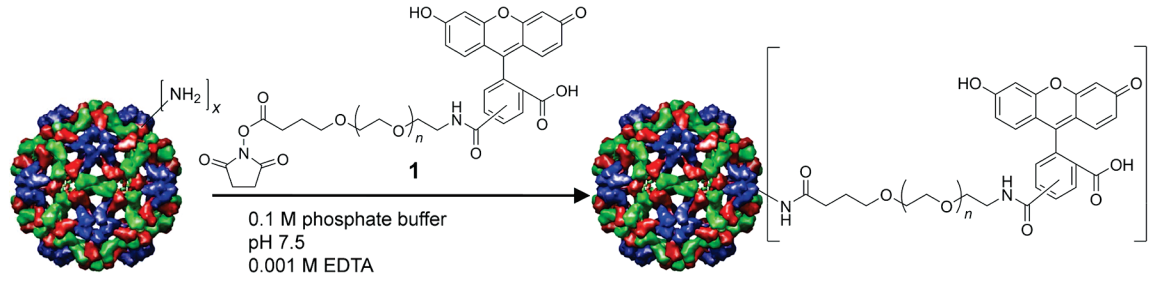

hybrids. The attachment of PEG chains was accomplished by mixing compound **1** with a solution of CCMV in phosphate buffer (pH 7.5) at various CP/PEG molar ratios (samples **A** (1:50), **B** (1:25), **C** (1:10), and **D** (1:1); Scheme 2).

The presence of virus−polymer conjugates was confirmed by UV/vis spectroscopy, fast protein liquid chromatography (FPLC), transmission electron microscopy (TEM), and gel electrophoresis (Figures 1 and S2). The FPLC chromatograms of all samples (**A**−**D**) showed peaks at a retention volume $V = 0.90$ mL, which is lower than the characteristic value for the virus under the same conditions ($V = 1.06$ mL; Figure 1a), suggesting the formation of larger particles. Experiments with PEG of other chain lengths have also been carried out (PEG-750 and PEG-10000). The functionalization reaction was successful in both cases. However, no significant changes in the FPLC chromatogram were observed for the derivatization with PEG-750, while precipitation seemed to occur when PEG-10000 was used. UV/vis spectra of fractions taken directly from the FPLC column at $V = 0.90$ mL showed absorption bands from both the polymer ($\lambda = 490$ nm, resulting from the fluorescein moiety) and the virus ($\lambda = 260$ nm, resulting from the viral RNA), proving the formation of polymer−virus conjugates (Figure S2a; the absorption maximum of the protein is located at $\lambda = 280$ nm, so this is the wavelength to be monitored, instead of $\lambda = 260$ nm, when empty capsids or disassembled protein subunits will be studied). The average number of PEG chains per protein subunit could be estimated from the ratio of these absorbance values, and a good correlation with the initial ratios of protein and polymeric material used in the reaction mixtures was observed. A maximum number of 2−3 PEG chains per protein subunit were found in the case of a 1:50 initial CP/PEG ratio (Figure 1b), which is in good agreement with the anticipated number of available amine groups on the exterior surface of CCMV. The SDS-PAGE results suggest that the degree of functionalization of the coat protein is similar for all samples **B**−**D** (Figure S2c), while sample **A** contains small amounts of protein having a higher degree of functionalization (Figure S2d). The varying ratios of PEG/CP observed in Figure 1b likely originate from differences in the amount of PEG-functionalized CP subunits in the conjugates rather than to their different degrees of functionalization. None of the used techniques showed evidence for the formation of CCMV-PEG conjugates in the control experiment.

During the characterization of samples **A**−**D** by FPLC, it was observed that a substantial decrease in the intensity of the peak at $V = 0.90$ mL occurred after successive injections of the same sample. It seemed from these data that the grafting of PEG chains onto the CCMV virus forced, to a certain degree, the disassembly of its capsid. To unravel the details and extent of this process, the stability of the CCMV-PEG assemblies was systematically studied over time. All samples showed the same behavior, therefore, only the results for sample **B** are shown in Figure 2. The mixture obtained after the reaction and the preliminary SEC purification (Sephadex G-100) was analyzed by FPLC at different times over a three week period. Besides the peak at $V = 0.90$ mL, two additional peaks were initially present in every FPLC chromatogram (Figure 2a), which seem to correspond to polymer aggregates ($V = 1.60$ mL) and the polymer itself ($V = 1.95$ mL; see the Supporting Information, page S15, for the assignment of these peaks). A decrease in the intensity of the peak at $V = 0.90$ mL, recorded by following the absorbance at $\lambda = 280$ nm, was observed in time (Figures 2b and S3). Simultaneously, the intensity of the peak at $V = 1.95$ mL increased, while the peak at $V = 1.65$ mL stayed constant. This result points to the disassembly of the conjugates into species that elute at similar retention volumes to the polymer.

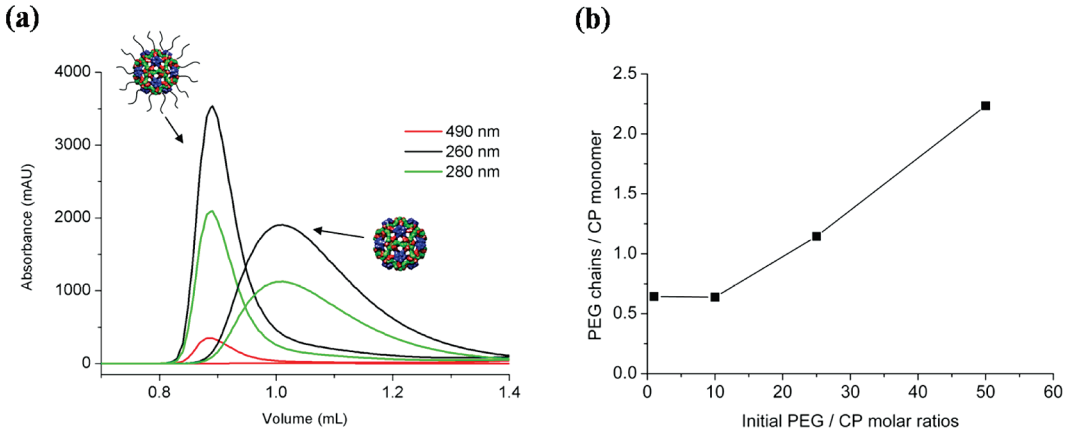

Figure 1. Analysis of the CCMV-PEG conjugates. (a) FPLC chromatograms of SEC-purified sample **B** (1:25), and wild-type CCMV under the same conditions of pH and ionic strength (detection at 280 nm, green; at 260 nm, black; and at 490 nm, red). (b) Plot showing the average number of PEG chains per CP subunit versus the initial PEG/CP molar ratios used to prepare the reaction mixtures.

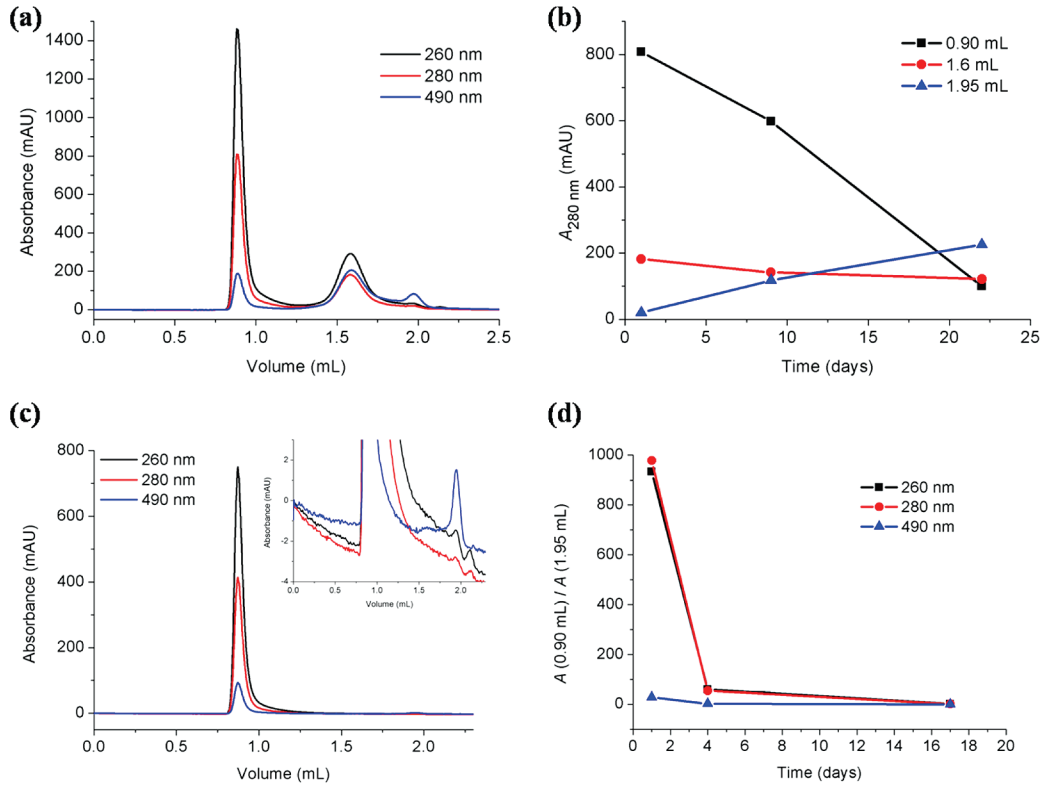

Figure 2. FPLC graphs as obtained for stability studies on sample **B** (sample was first purified on Sephadex G-100). (a) FPLC chromatogram after 1 day. (b) Absorbance at $\lambda = 280$ nm as a function of time for the different peaks observed after injection of sample **B**. (c) FPLC chromatogram of the reinjected fraction at $V = 0.90$ mL in (a) one day after the first injection. Inset: magnification of the peak at $V = 1.95$ mL. (d) Plot of the ratio of intensities of peaks at $V = 0.90$ and 1.95 mL for the reinjected fraction as a function of time.

Scheme 3. Tentative Scenario Proposed for the Disassembly of CCMV-PEG Conjugates into CP Bearing PEG Chains and Nonfunctionalized CP

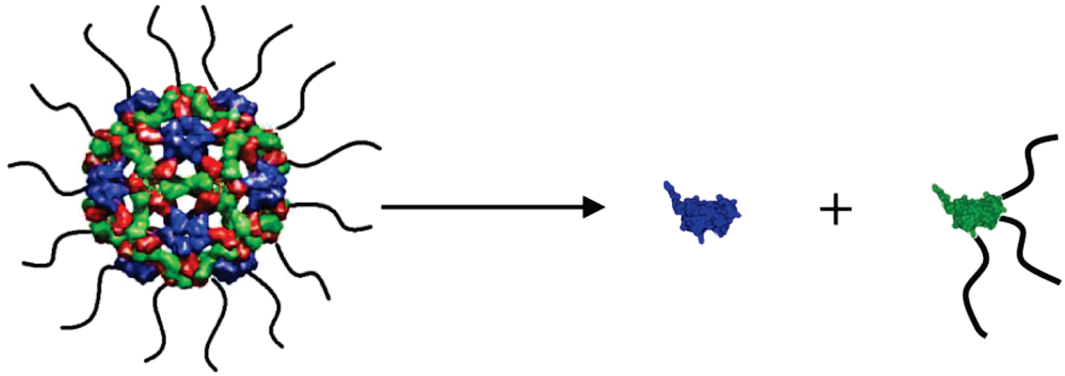

To obtain more insight into the disassembly process, the fraction at $V = 0.90$ mL from the FPLC chromatogram in Figure 2a, which contains the pure CCMV-PEG conjugates, was also reinjected at different time intervals. The evolution of the pure CCMV-PEG conjugates in time showed the same tendency as observed for the original samples **A**−**D**. Whereas only the peak associated with the conjugates ($V = 0.90$ mL) appeared in the FPLC chromatograms after one day (Figure 2c), the intensity of this peak rapidly decreased over time, concomitantly with the formation of a new peak at $V = 1.95$ mL (Figure S4). This process can be illustrated by plotting the ratio of intensities of both peaks at various wavelengths as a function of time (Figure 2d). Analysis by SDS-PAGE, UV/vis, and infrared spectroscopy confirmed the presence of both protein and polymer in the fraction corresponding to this new peak (Figures S6). The elution volume of the peak is larger than the one of the nonfunctionalized CP dimers ($V = 1.78$ mL), suggesting that PEG-functionalized CP monomers and not dimers are generated during the disassembly. Nevertheless, it cannot be excluded that the peak consists of both functionalized and nonfunctionalized CP subunits. It should be noted that what is being referred to as PEG-functionalized CP monomers actually implies species that can have 0−3 PEG chains per protein subunit.

The whole set of experiments suggests a scenario for the disassembly of CCMV-PEG conjugates, as depicted in Scheme 3. The slow but irreversible dissociation of the CCMV-PEG conjugates is probably a consequence of the disruption of protein−protein interactions caused by steric interference due to the presence of the PEG chains. The influence that organic substituents can exert on the assembly of viral capsids has previously been studied for the hepatitis B virus (HBV), the assembly process of which was misdirected to the formation of much larger particles than that of the native virus.[38] The stability studies described above provide more information on this kind

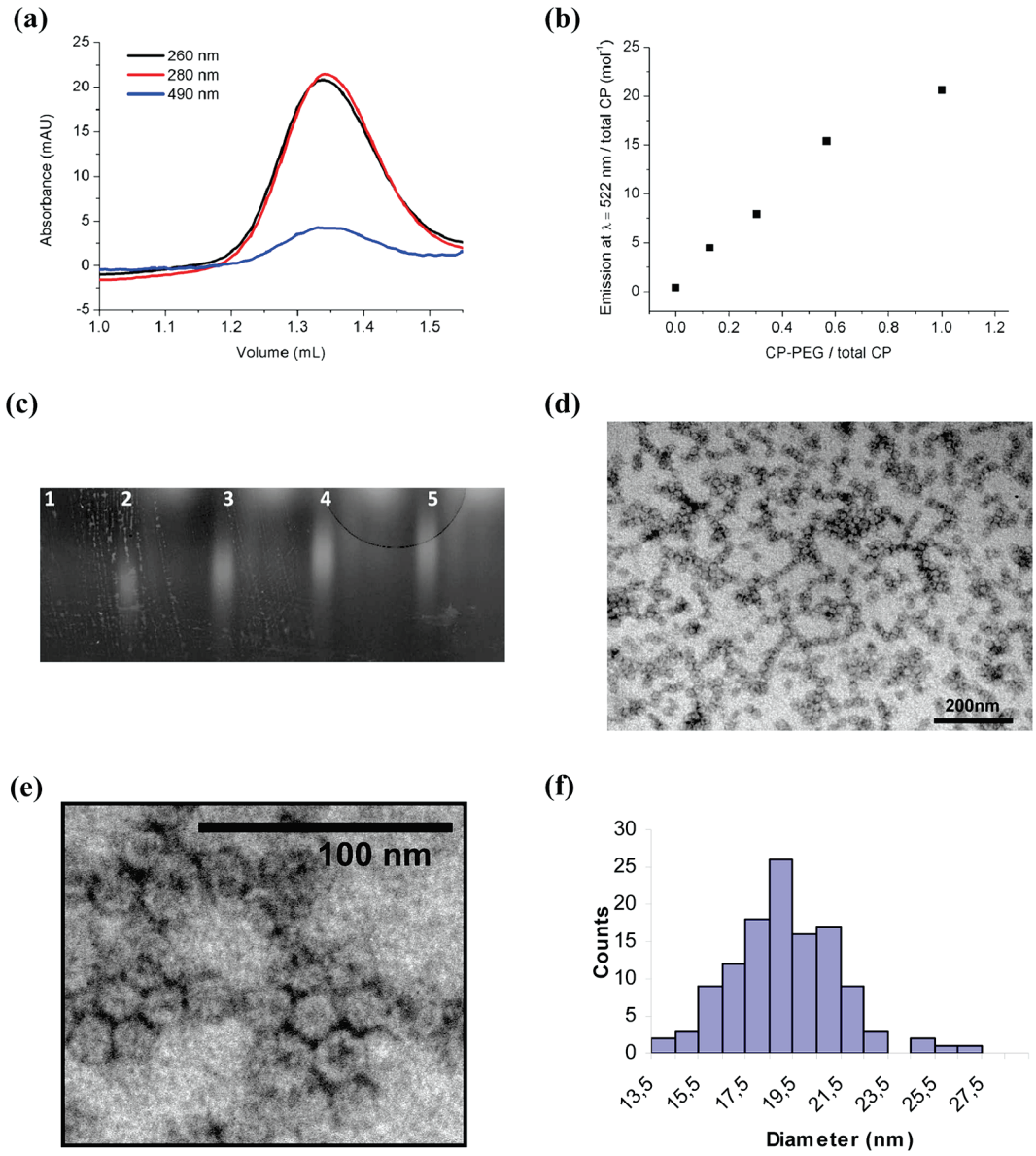

Figure 3. (a) FPLC chromatogram of the PSS-CCMV-PEG assemblies formed using 100% PEG-CP (sample **I**). (b) Emission at $\lambda = 522$ nm ($\lambda_{exc} = 490$ nm) of the FPLC fractions at $V = 1.35$ mL plotted versus the amount of PEG-CP used for the assembly in samples **E**−**I**. (c) Agarose gel of pure PSS-CCMV-PEG $T = 1$ particles (purified by FPLC) bearing different amounts of PEG chains: 0 (lane 1), 25 (lane 2), 50 (lane 3), 75 (lane 4), and 100% PEG-CP (lane 5). The gel was visualized with a fluorescence scanner. (d) TEM micrograph of the PSS-CCMV-PEG $T = 1$ particles, taken from sample **G** (50% PEG-CP). (e) Zoom in on the TEM micrograph shown in (d). (f) Size distribution of the PSS-CCMV-PEG $T = 1$ particles shown in (d).

of phenomenon. The tendency of the CCMV-PEG conjugates to dissociate should be taken into account as a very likely side process, if one aims to decorate CCMV with organic polymers. The potential instability of these CCMV assemblies, however, does not exclude further experiments, as described below.

Assembly of PSS-CCMV-PEG Virus-like Particles. Before studying the reassembly of the PEG-functionalized coat proteins into virus-like particles, the RNA still present had to be removed. Dialysis of samples **A**−**D** against Tris-HCl buffer (pH 7.5, 1.0 M NaCl) allowed the viral genomic material to precipitate. After ultracentrifugation and collection of the supernatant, the samples were free from RNA, as evidenced by the absence of its characteristic absorption at $\lambda = 260$ nm (Figure S7a). SDS-PAGE analysis revealed that both functionalized and nonfunctionalized CP subunits were isolated (Figure S7b). Furthermore, it could be concluded from their high elution volume in the FPLC chromatograms of the supernatant (Figure S7c) that the CP subunits were still present in their monomeric form.

By following the approach described by Sikkema et al.,[32] the isolated PEG-functionalized coat proteins were reassembled using PSS (MW = 70000 g mol^{-1}) as the template. The assembly was performed at pH 7.5 with a ratio of approximately 15 PSS repeating units per coat protein, which is within the optimal range of values described for the formation of $T = 1$ particles (considering that there are 8−9 cationic residues in the N-terminus of each coat protein subunit, 2 equiv of PSS repeating units are approximately being used). One interesting question is what effect the presence of PEG chains attached to the protein has on the assembly process. A suitable way to evaluate this would be to assemble mixtures that have different compositions of functionalized and nonfunctionalized CP to test the extent to which the particles are formed as well as their degree of coverage with PEG chains. To this end, five different mixtures of CP and PEG-CP (samples **E**−**I**, containing 0, 25, 50, 75, and 100% PEG-CP, respectively), in the presence of

PSS, were prepared and studied. The nonfunctionalized CP was prepared as described in the literature.[16,39,40]

After mixing the components of samples **E**−**I** at pH = 7.5 and incubating for 30 min at room temperature, the mixtures were purified by FPLC chromatography and further analyzed by fluorescence spectroscopy, SDS-PAGE, and TEM (Figure 3). A peak at $V = 1.35$ mL in the FPLC chromatograms indicated the formation of $T = 1$ particles for the various CP/PEG-CP ratios employed in the experiment (Figure 3a). All samples gave similar chromatograms, which only differed in the intensity of this peak at different wavelengths (Figure S8). Moreover, the presence of absorbance at $\lambda = 280$ and 490 nm demonstrated that both the coat protein and polymer were constituents of the material eluting at $V = 1.35$ mL. This was further confirmed by the fluorescence spectrum of this FPLC fraction, which showed a clear emission at $\lambda = 520$ nm when excited at $\lambda = 490$ nm (Figure S9). On the contrary, no absorption at $\lambda = 490$ nm and fluorescence at $\lambda = 520$ nm were detected for sample **A**, which contained no PEG-CP. In addition to the peak at $V = 1.35$ mL, there was the elution at higher volumes in the chromatograms of other material (Figure S8). The nature of this material is as yet unknown, although it probably consists of highly PEG-functionalized CP monomers and residual polymer that are not able to assemble around the PSS.

Interestingly, the FPLC chromatograms of samples **E**−**I** did not change over time. It therefore seems that the PSS-CCMV-PEG particles are more robust than their CCMV-PEG conjugate predecessors. The particles were also found to be stable at pH 5.0 as dialysis against an acetate buffer at this pH value did not lead to substantial changes in the FPLC results (Figure S10). The electrostatic interactions between the negative charges of PSS and the positively charged N-terminus of the coat protein molecules are likely to be the reason for this remarkable increase in robustness.

The degree of coverage of the PSS-CCMV-PEG particles with PEG chains, when using different CP/PEG-CP ratios, was evaluated by plotting the emission at $\lambda = 522$ nm ($\lambda_{exc} = 490$ nm) of the FPLC fractions at $V = 1.35$ mL, normalized to the total concentration of coat proteins present, versus the amount of PEG-CP used in the initial assembly mixture. An almost linear relationship was obtained showing that the incorporation of PEG onto the $T = 1$ capsids is statistical (Figure 3b).

Samples **E**−**I** and their FPLC fractions at $V = 1.35$ mL were further characterized by agarose gel electrophoresis (Figure 3c). The gel was visualized with the help of a fluorescence scanner in order to detect the fluorescein-labeled PEG chains. The FPLC fractions showed single bands running faster than the band of the wild-type virus (Figure S11), as expected for smaller particles. The fact that these bands are visible by fluorescence is a strong proof that PEG is present on the outside of the $T = 1$ capsids (note the absence of such a band in the case of sample **E**, 0% PEG-CP, lane 1). The degree to which PEG-functionalization of the particles occurred could even be inferred from the dependence of their running speed in the gel on the initial amount of PEG-CP used in the assembly mixtures.

Finally, the PSS-CCMV-PEG particles were studied by TEM (Figure 3d−f). This study confirmed that the particles are monodisperse spherical capsids with an average diameter of 18.5 nm. The particles showed a slightly larger size than the $T = 1$ particles reported by Sikkema et al.,[32] probably caused by the presence of the PEG tails attached to the outer surface of the protein cage.

Conclusion

Based on its reversible pH-dependent disassembly/assembly behavior, the CCMV capsid is a suitable nanocontainer for the encapsulation of proteins, inorganic nanoparticles, and organic polymers.[19] The external functionalization of these capsids with synthetic organic polymers will broaden the field of potential application, for example, as nanoreactors and as nanostructured materials. We have shown that the covalent attachment of polymer tails to the outer surface of the CCMV capsid leads to some thermodynamic instability that forces the virus to disassemble over a period of days. The irreversible dissociation of CP dimers, probably due to steric interference between the protein−protein subunits as a result of the proximity of the PEG chains, is responsible for the shift of the equilibrium to complete disassembly of the viral particles. This limits the potential application of the CCMV−polymer biohybrids, however, this can be overcome if a polystyrene sulfonate guest is present in the modified viral capsids. The methodology described here allows for complete control over the amount of PEG chains attached to the PSS-CCMV-PEG particles. Moreover, there is a remarkable increase in their robustness compared with the CCMV-PEG conjugates, an important requirement if VLPs are to be used in nanotechnology. The polymers chosen for this work are not yet functional, but the approach exemplifies a possible future strategy for the design and preparation of more sophisticated VLPs. Any negatively charged synthetic polymer could in principle be used as a template to direct the viral capsid assembly toward the formation of stable and precisely defined architectures. The use of functional polymers both inside and outside of the capsids would impart new properties to the particles. Our strategy implies that these properties can be tuned by the proper choice of the external polymer and the template.

Acknowledgment. We thank the IEF Marie Curie program of the European Union (A.E.), the Chemical Council of The Netherlands Organization for Scientific Research, the research school NRSC-Catalysis (A.J.D.), the Royal Netherlands Academy of Arts and Sciences (J.J.LM.C. and R.J.M.N.), and the European Science Foundation (ESF) EURYI program (J.J.L.M.C.) for financial support.

Supporting Information Available. Synthetic procedures and characterization of CCMV-polymer biohybrids. This material is available free of charge via the Internet at http://pubs.acs.org.

References and Notes

(1) Niemeyer, C. M. *Angew. Chem., Int. Ed.* **2001**, *40*, 4128–4158.
(2) Rotello, V. M. *J. Mater. Chem.* **2008**, *18*, 3739–3740.
(3) Douglas, T.; Young, M. *Science* **2006**, *312*, 873–875.
(4) Fischlechner, M.; Donath, E. *Angew. Chem., Int. Ed.* **2007**, *46*, 3184–3193.
(5) Uchida, M.; Klem, M. T.; Allen, M.; Suci, P.; Flenniken, M.; Gillitzer, E.; Varpness, Z.; Liepold, L. O.; Young, M.; Douglas, T. *Adv. Mater.* **2007**, *19*, 1025–1042.
(6) Wang, Q.; Lin, T.; Tang, L.; Johnson, J. E.; Finn, M. G. *Angew. Chem., Int. Ed.* **2002**, *41*, 459–462.
(7) Sen Gupta, S.; Kuzelka, J.; Singh, P.; Lewis, W. G.; Manchester, M.; Finn, M. G. *Bioconjugate Chem.* **2005**, *16*, 1572–1579.
(8) Young, M.; Willits, D.; Uchida, M.; Douglas, T. *Annu. Rev. Phytopathol.* **2008**, *46*, 361–384.
(9) Vriezema, D. M.; Comellas Aragones, M.; Elemans, J. A. A. W.; Cornelissen, J. J. L. M.; Rowan, A. E.; Nolte, R. J. M. *Chem. Rev.* **2005**, *105*, 1445–1489.
(10) Yamashita, I. *J. Mater. Chem.* **2008**, *18*, 3813–3820.
(11) Ueno, T.; Suzuki, M.; Goto, T.; Matsumoto, T.; Nagayama, K.; Watanabe, Y. *Angew. Chem., Int. Ed.* **2004**, *43*, 2527–2530.

(12) Ensign, D.; Young, M.; Douglas, T. *Inorg. Chem.* **2004**, *43*, 3441–3446.
(13) Tominaga, M.; Ohira, A.; Kubo, A.; Taniguchi, I.; Kunitake, M. *Chem. Commun.* **2004**, 1518–1519.
(14) Varpness, Z.; Peters, J. W.; Young, M.; Douglas, T. *Nano Lett.* **2005**, *5*, 2306–2309.
(15) Abe, S.; Niemeyer, J.; Abe, M.; Takezawa, Y.; Ueno, T.; Hikage, T.; Erker, G.; Watanabe, Y. *J. Am. Chem. Soc.* **2008**, *130*, 10512–10514.
(16) Comellas-Aragones, M.; Engelkamp, H.; Claessen, V. I.; Sommerdijk, N. A. J. M.; Rowan, A. E.; Christianen, P. C. M.; Maan, J. C.; Verduin, B. J. M.; Cornelissen, J. J. L. M.; Nolte, R. J. M. *Nat. Nanotechnol.* **2007**, *2*, 635–639.
(17) Johnson, J.; Lin, T.; Lomonossoff, G. *Annu. Rev. Phytopathol.* **1997**, *35*, 67–86.
(18) Steinmetz, N. F.; Lin, T.; Lomonossoff, G. P.; Johnson, J. E. *Curr. Top. Microbiol. Immunol.* **2009**, *327*, 23–58.
(19) de la Escosura, A.; Nolte, R. J. M.; Cornelissen, J. J. L. M. *J. Mater. Chem.* **2009**, *19*, 2274–2278.
(20) Schlick, T. L.; Ding, Z.; Kovacs, E. W.; Francis, M. B. *J. Am. Chem. Soc.* **2005**, *127*, 3718–3723.
(21) Raja, K. S.; Wang, Q.; Gonzalez, M. J.; Manchester, M.; Johnson, J. E.; Finn, M. G. *Biomacromolecules* **2003**, *4*, 472–476.
(22) Wang, Q.; Raja, K. S.; Janda, K. D.; Lin, T.; Finn, M. G. *Bioconjugate Chem.* **2003**, *14*, 38–43.
(23) Steinmetz, N. F.; Manchester, M. *Biomacromolecules* **2009**, *10*, 784–792.
(24) Kovacs, E. W.; Hooker, J. M.; Romanini, D. W.; Holder, P. G.; Berry, K. E.; Francis, M. B. *Bioconjugate Chem.* **2007**, *18*, 1140–1147.
(25) Pasut, G.; Veronese, F. M. *Adv. Polym. Sci.* **2006**, *192*, 95–134.
(26) Harris, J. M.; Chess, R. B. *Nature Rev. Drug Discovery* **2003**, *2*, 214–221.
(27) Aniagyei, S. E.; DuFort, C.; Kao, C. C.; Dragnea, B. *J. Mater. Chem.* **2008**, *18*, 3763–3774.
(28) Speir, J. A.; Munshi, S.; Wang, G. J.; Baker, T. S.; Johnson, J. E. *Structure* **1995**, *3*, 63–78.
(29) Johnson, J. E.; Speir, J. A. *J. Mol. Biol.* **1997**, *269*, 665–675.
(30) Douglas, T.; Young, M. *Nature* **1998**, *393*, 152–155.
(31) de la Escosura, A.; Verwegen, M.; Sikkema, F. D.; Comellas-Aragones, M.; Kirilyuk, A.; Rasing, T.; Nolte, R. J. M.; Cornelissen, J. J. L. M. *Chem. Commun.* **2008**, 1542–1544.
(32) Sikkema, F. D.; Comellas-Aragones, M.; Fokkink, R. G.; Verduin, B. J.; Cornelissen, J. J. L. M.; Nolte, R. J. M. *Org. Biomol. Chem.* **2007**, *5*, 54–57.
(33) Hu, Y. F.; Zandi, R.; Anavitarte, A.; Knobler, C. M.; Gelbart, W. M. *Biophys. J.* **2008**, *94*, 1428–1436.
(34) Bancroft, J. B.; Hills, G. J.; Markham, R. *Virology* **1967**, *31*, 354–379.
(35) Bruinsma, R. F.; Gelbart, W. M.; Reguera, D.; Rudnick, J.; Zandi, R. *Phys. Rev. Lett.* **2003**, *90*, 248101.
(36) Tang, J.; Johnson, J. M.; Dryden, K. A.; Young, M. J.; Zlotnick, A.; Johnson, J. E. *J. Struct. Biol.* **2006**, *154*, 59–67.
(37) Mukherjee, S.; Pfeifer, C. M.; Johnson, J. M.; Liu, J.; Zlotnick, A. *J. Am. Chem. Soc.* **2006**, *128*, 2538–2539.
(38) Stray, S. J.; Bourne, C. R.; Punna, S.; Lewis, W. G.; Finn, M. G.; Zlotnick, A. *Proc. Natl. Acad. Sci. U.S.A.* **2005**, *102*, 8138–8143.
(39) Verduin, B. J. M. *FEBS Lett.* **1974**, *45*, 50–54.
(40) Verduin, B. J. M. *J. Gen. Virol.* **1978**, *39*, 131–147.
(41) Gillitzer, E.; Willits, D.; Young, M.; Douglas, T. *Chem. Commun.* **2002**, 2390–2391.
(42) http://viperdb.scripps.edu/index.php.

BM9007953